New observations of displacement steps associated with volcano seismic long-period events, constrained by step-table experiments

Johannes Thun,[1] Ivan Lokmer,[1] Christopher J. Bean[1]

Corresponding author: J. Thun, School of Geological Sciences, University College Dublin, Belfield, Dublin 4, Ireland. (johannes.thun@ucdconnect.ie)

[1]Seismology Laboratory, School of Geological Sciences, University College Dublin, Ireland.

Long period (LP) volcano seismic events often precede volcanic eruptions and are viewed with considerable interest in hazard assessment. They are usually thought to be associated with resonating fluid-filled conduits although alternative models involving material failure have recently been proposed. Through recent field experiments, we uncovered a step-like displacement component associated with some LP events, outside the spectral range of the typically narrow-band analysis for this kind of event. Bespoke laboratory experiments with step tables show that steps of the order of a few micrometres can be extracted from seismograms, where long period noise is estimated and removed with moving median filters. Using these constraints, we observe step-like ground deformation in LP recordings near the summits of Turrialba and Etna volcanoes. This represents a previously unobserved static component in the source time history of LP events, with implications for the underlying source process.

1. Introduction

The investigation of seismic events on volcanoes plays a major role in enhancing our understanding of volcanic systems, as they carry information on the dynamics of the volcanic edifice and its plumbing system. Long-period (LP) and very long period (VLP) seismic events are of particular importance, as their occurrence is often thought to be directly associated with magmatic and/or hydrothermal processes [e.g. *Chouet*, 2003, and references therein] and if so, could give information on the volcanic plumbing systems and changes in volcanic activity. According to the classification of LP events given by *Chouet* [2003] typical LP events contain frequencies between 0.5 Hz and 5 Hz, although *McNutt* [2005] pointed out significant changes with time and between different volcanoes. In the data recorded on Mt Etna, Sicily [*Lokmer et al.*, 2008] and Turrialba, Costa Rica [*Eyre et al.*, 2013], we observed additional low energy spectral content well below these typical frequencies. This observation can have significant implications for our understanding of the nature of source time functions (STFs).

STFs from LP source inversions are often explained by fluid-filled cavity models proposed e.g. by *Chouet* [1986] and *Neuberg et al.* [2000]. In these models, slow waves travel at the fluid-solid interface and their interference can cause sustained resonance observed at the surface [*Chouet*, 1986; *Ferrazzini and Aki*, 1987]. Full waveform inversions of LP events have been implemented in studies on several volcanoes, with results often interpreted within the scope of such models [e.g. *Legrand et al.*, 2000; *Kumagai*, 2002; *Nakano et al.*, 2003; *Kumagai et al.*, 2005; *Lokmer et al.*, 2007; *Cusano et al.*, 2008; *De Barros et al.*, 2011; *Eyre et al.*, 2013]. It is important to note that the waveforms used in these

inversions were band-pass filtered. Recent observations in the summit region [e.g. Fig. 2b in *Lokmer et al.*, 2007; *Bean et al.*, 2014; *Eyre et al.*, 2015] show impulsive waveforms associated with LP events. *Bean et al.* [2014] and *Eyre et al.* [2015] demonstrated that resonance observed on seismograms can be a consequence of wave propagation in poorly consolidated materials for stations more than about 1 km from the source. Consequently, *Bean et al.* [2014] proposed an alternative model, where shallow LP events are a consequence of slow rupture within the volcanic edifice. *Eyre et al.* [2015] showed that this source model can explain LP event waveforms recorded on Turrialba volcano.

The current processing practice of filtering LP events within the most energetic frequency band prior to inversions means that most of the LP sources interpreted in the literature are band-pass filtered representations of the true source-time histories. In our unfiltered integrated field data we recently observed small apparent displacement steps in the near-field of individual LP events. If this observation is real, it could significantly contribute to our understanding of LP sources. However, we are aware of problems associated with tilt, long period instrumental and environmental noise and microseisms contaminating the records. Here we quantify step displacement recovery from broadband seismic data using step table laboratory experiments. We then apply a data processing method to recover displacement steps in exemplary near field LP signals from Turrialba and Etna volcanoes.

2. Seismometers as deformation sensors?

Our recent near-field observations ($\leq 1-2$ km from estimated source locations) indicate that the frequency content of LP events may in some cases extend all the way down to

zero frequency, namely corresponding to a displacement step. To our knowledge, this is the first such observation, although small displacements steps (possibly of the order of micrometres) can be expected for some LP source models [e.g. *Bean et al.*, 2014; *Eyre et al.*, 2015]. In strong-motion seismology, static displacements associated with earthquakes are recovered from accelerometer data [e.g. *Graizer*, 2005; *Chanerley et al.*, 2013], although it is a difficult task and displacements are often not entirely recoverable. The signal-to-noise ratio (SNR) in these scenarios is typically much higher than for the waveforms associated with volcanic LP events.

If we seek to recover ground displacement steps from seismograms, we need to address long-period dynamic noise as well as other long-period signals (e.g. from tilt) contaminating the records. The influence of tilt motions on horizontal components of inertial seismometers has been known for a long time [e.g. *Rodgers*, 1968; *Graizer*, 2005; *Pillet and Virieux*, 2007]. For small signals and neglecting the terms for angular acceleration and cross-axis sensitivity, the differential equation describing a horizontal pendulum is:

$$\ddot{y}_1 + 2\omega_1 D_1 \dot{y}_1 + \omega_1^2 y_1 = -\ddot{x}_1 + g\psi_2 \tag{1}$$

where x_1 and y_1 are ground displacement and the pendulum response, respectively; ω_1 and D_1 the natural frequency and critical damping of the pendulum, respectively; g is the gravitational acceleration and ψ_2 the ground rotation around the second horizontal axis, i.e. tilt in x_1-direction [for details see *Graizer*, 2005]. Here we see that tilt has a first order effect on the horizontal pendulum, which can in fact become dominant at long periods (e.g. above 10 s). Currently available tilt meters on the other hand, are also susceptible to translational motion in the LP (e.g. 0.5 - 5 Hz) frequency range [*Fournier*

et al., 2011]. Hence with current instrumentation we cannot fully distinguish tilt motion from translational motion. Until real rotational sensors that can be deployed in a field setting are developed [e.g. *Schreiber et al.*, 2006], other ways of dealing with tilt have to be adopted.

The equation for the vertical response looks similar to equation (1), but the last (rotational) term can be neglected, which means the vertical component seismograms are not sensitive to small tilts. *Wielandt and Forbriger* [1999] used this difference between vertical and horizontal components to separate translational and rotational contributions on horizontal seismograms in the near-field of an assumed isotropic source. In general this property makes a displacement step recovery from vertical recordings a lot more straightforward and less ambiguous than from horizontal components.

3. Laboratory Experiments

Integrated seismometer data offers displacement information. However a seismometer's response filters true ground motion - by design seismometers lose sensitivity in the limit of zero frequency. Consequently, instrument noise starts to dominate for longer periods. Displacement steps (i.e. one-sided positive or negative velocity pulses) have a broad spectrum, including static (or zero) frequencies. Here we assess the degree to which displacement steps can be recovered from broadband seismometer data. We carried out laboratory experiments in which we exposed seismometers to well-defined steps, using a Lennartz CT-EW1 step table, which can achieve vertical steps as small as $\sim 90\,\mu$m with high precision. The displacement time history varies between 0.5 s and 2.5 s, depending on table setting and load. In addition, we designed and built a simple customized step table

(Figure 1c), which does not have the same precision as the calibration table, but allows for an arbitrary displacement time history. The displacement is driven by manual operation of a micrometer screw and its value can be read directly from the screw's scale, with a resolution of 10 μm. It is directed at a 45° angle with respect to the ground, resulting in equivalent displacements in upwards and horizontal directions. Tilting of the table with angles of the order of about 10 microradians cannot be avoided in this setup and has to be kept in mind especially when analysing horizontal recordings. However, in comparison to tilt steps measured on volcanoes (typically a few orders of magnitude smaller), these signals are large and serve as an upper limit for tilt contamination of field data.

3.1. Vertical Component

Figure 1a shows the integrated vertical seismograms, i.e. displacements, of a 94 μm upward step (black: ramp time 0.6 s; red: 1.8 s ramp with added noise, see below), recorded by a Guralp 3ESPCD (60 s) instrument on the Lennartz table. The uppermost plot shows unprocessed, integrated seismograms, which is approximately the instruments' impulse response, acting as a causal high-pass filter. In the second panel, the instrument response was removed without additional filters. The step is now clearly visible in the data, but amplified (very) long period noise is also present. During the deconvolution of the instrument response, high-pass filters are routinely applied in order to deal with this noise. Hence, the third plot shows the effect of an acausal high-pass filter with the corner frequency of 0.01 Hz. Whilst it reduces long period noise, it also alters the step waveform significantly by removing its low-frequency portion. For higher filter frequencies (note that the typical lower LP filter corner of 0.3 Hz is about 5 octaves above 0.01 Hz) the step waveform is

completely masked by the filter and cannot be distinguished from a dynamic motion. We assessed other filtering methods and found moving median filters suitable for the task of step recovery. Similar to moving average filters, we take the median of a window of width M around each data point x_n:

$$x_n^M = \text{Median}\left(x_{n-\frac{M}{2}f_s}, \ldots, x_{n+\frac{M}{2}f_s}\right) \tag{2}$$

where f_s is the sampling frequency and M is given in seconds. The filter is used to estimate the long-period noise of the velocity record and is insensitive to transient signals with durations significantly shorter than half the window length. As high frequency noise, tremor or other signal components can impede noise estimation with the (non-linear) moving median filter, a low-pass filter is applied to the instrument corrected data. A corner frequency of $f_c = 5/M$ was found suitable. The noise estimate is then subtracted from the original unfiltered, instrument corrected velocities and the result integrated to get displacements. The outcome for the previous lab example, using a moving median filter with $M = 30\,\text{s}$ is shown in the lowermost panel of Figure 1a, where the step waveform is successfully recovered from the seismogram. The misfit of the step estimation is:

$$\Delta_{\text{step}} = \frac{u_{\text{measured}} - u_{\text{real}}}{u_{\text{real}}} = \frac{102\,\mu\text{m} - 94\,\mu\text{m}}{94\,\mu\text{m}} = 0.085, \tag{3}$$

i.e. the amplitude of the step is overestimated by 8.5 %. In comparison to field observations, the SNR in the experiment is very high and the rise time of the step is quite short (0.6 s). We thus used the recording of a slower step (i.e. a smaller velocity pulse) from the same table (1.8 s rise time) and added noise recorded on Turrialba summit station CIMA (red lines in Figure 1a). The noise was amplified in order to match SNRs observed on Turrialba (see Section 4). The resulting displacements show that for SNRs similar to

our Turrialba field data, the step is still well recovered with a misfit of $\Delta = 0.053$, i.e. overestimated by about 5 %. Comparing different noise levels added to step table data, we estimate that the method's detection threshold for steps lies at about 1 μm for a 3ESPCD instrument. This corresponds to approximately 5 times the root-mean-square amplitude of the displacement noise below 2 Hz.

As the Lennartz table is restricted to vertical motion and limited step rise times, we tested the performance of the processing on different ramp lengths using our customized step table. We exposed the same instrument to steps of about 100 μm (about 70 μm in vertical and north directions of the instrument), altering ramp times between 0.6 s and 20 s. We applied the processing described above, with varying median filter windows to recordings of different ramps (Figure 1b). The grey area shows the actual displacement, including an assumed error of about $\pm$10% (based on reading precision at the micrometer screw). The results shown in Figure 1b confirm that stable results are achieved as long as the filter window M is chosen accordingly. We recommend a window length of about three times the ramp time. As in practice the ramp time is unknown, the signal length inferred from raw displacements can be a good starting point. If the length of the filter window is not sufficient for a given signal, it can strongly affect the recovered step. On the other hand, if the step is real, the recovered value is stable over a wide range of M (Figure 1b). Hence, we explore different windows M, starting at 3 times the signal length and gradually increasing M by 5 s each time until we achieve a robust solution with satisfactory noise removal. For now, this manual process is necessary to ensure stability and robustness of the results. There is no upper limit for the choice of M, but as filter

windows get longer, less noise can be removed. Consequently, the method is limited by the SNR.

3.2. Horizontal Components

Our customized table displaces the instrument horizontally to the same extent as vertically due to its 45° angle of translation with respect to the ground. During the displacements, driven by turning the micrometer screw, the table surface is tilted uncontrollably, a problem that cannot be avoided when creating horizontal displacements with this setup. This tilt leads to a long period transient dominating the horizontal seismograms (see dashed line in Figure 1d), but negligible on the vertical component. Associated with the displacements, we measure steps of about 1 to $20 \cdot 10^{-6}$ g in instrument corrected and differentiated (i.e. acceleration) seismograms. According to the tilt term in Equation 1 this corresponds to tilt steps of about 1 to 20 μrad. Tilts this strong make it difficult to extract displacement steps from the horizontal seismograms, but do not interfere with recovery on the vertical component, as shown above. However, the tilts observed in our field experiments on volcanoes, where there are any, are several orders of magnitude smaller and thus do not create significant transients. A tilt step of the order of a few microradians would be directly visible particularly as a major waveform difference between vertical and horizontal components (see above and Figure 1d).

As the instrument in our experiment sits directly on the source and the tilt signal is negligible on the vertical component, the assumptions underlying the tilt separation method of *Wielandt and Forbriger* [1999] are fulfilled. We thus applied this method to the data for the fastest step (0.6 s with $u_x = u_z \approx 70\mu$m), where a tilt of about 14 μrad

affected the north component, while the displacement in this direction was identical to the upward motion. The horizontal raw velocity seismogram (Figure 1d, dashed red line) shows a long-period transient, the seismometer's response to a tilt/acceleration step [for details see *Kinoshita*, 2008]. The tilt separation method was carried out between 0.005 Hz and 1 Hz, which exceeds the band suggested by *Wielandt and Forbriger* [1999] (0.005 Hz - 0.05 Hz), but works well here due to the high SNR. The solid line shows the resulting seismograms, in which the estimated tilt has been removed. Although the method's fit for this extreme (large tilt) example is not ideal (energy of the residual is about 8% of the original trace), it reduces the tilt transient significantly and thus exposes the velocity pulse. The lower panel in Figure 1d shows the displacement seismograms after application of the median filter method. Whilst without tilt reduction, the step is not retrieved on the horizontal component (dashed line), it is successfully recovered when tilt was reduced before median filter application. Both vertical and horizontal displacements show a step of about 77 μm, which is in good agreement with the known displacement (70 μm) in the presence of such large tilt contamination.

In conclusion, we demonstrate that static displacement steps can be recovered from seismometers when long-period noise is carefully addressed. Running median filters are a suitable tool to reduce this noise adequately, although strong tilt contamination on horizontal components may have to be dealt with separately. A summary of the steps and a Python code for the median filter can be found in the Supporting Information to this paper. Although we did not test this for instruments other than the aforementioned Guralp 3ESPCD (60 s; 2 x 3000 V/(m/s)) and a Guralp 6TD (30 s; 2 x 1200 V/(m/s)),

in principle any broadband seismometer should be suitable for step recovery, as long as the response is well known and can be removed accurately. In our tests, the (shorter period and less sensitive) 6TD instrument showed a lower SNR at long periods than the 3ESPCD type, posing a problem for small signals. Low instrumental noise at long periods is thus desirable. In the following we apply the constraints found in this section to field observations on volcanoes.

4. Applications to Field Data

Figure 2b shows the vertical seismogram of an LP event recorded on Turrialba in 2009 by the summit station CIMA (map in Figure 2a), using the same instrument type that we used in the laboratory (Guralp 3ESPCD 60 s). Here we compare the classical LP band pass filtered trace to the one processed with the median filter. In both cases, a low pass filter with a corner frequency of 4 Hz was applied in advance. While the velocity seismograms do not show a significant difference, the displacements show a clear step when processed with the median filter; this displacement step cannot be seen when data are filtered with the bandpass filter, as is common practice. As the rise time of the step, starting at about 6.5 s, is not longer than about 2 s, the 20 s median filter window applied in Figure 2b is in accordance with the results from the laboratory experiments.

This step behaviour is not singular to this LP event, but can be observed for multiple events in the 2009 catalogue. Figure 2c shows seismograms of a family of 183 events (from family 2 in *Eyre et al.* [2013]) and a stack of these. Here the data were corrected for instrument response and trend, but no further filters were applied. The data were normalised to match the peak-to-peak amplitudes between events. Although (due to

strong long-period noise) only some single events show a clear static displacement like in Figure 2b, the integrated stack of this family shows a pronounced step, even without applying a median filter. This shows that this step-like behaviour is coherent across LP events and can be detected when recorded in the near field at the summit of Turrialba. The same behaviour was observed at a second summit station CIM2 (Figure 2a), using the same instrumentation. Shorter period instrumentation and greater distances from the summit lead to sparse observation of such steps at other locations during the same field experiment.

On Mt Etna, Italy, similar step-like behaviour can be observed on broadband station ECPN (Nanometrics Trillium 40 s) near the summit area (map in Figure 3a). Here, the step is embedded within a clear very long period signal which is coherent in waveform shape and size across many LP events recorded in 2005. Figure 3b shows displacements for 17 of these events and their stack. The filtered stack for the main energy peak of the event (0.3 - 1.3 Hz) shows the typical filtered waveform that is normally used for LP waveform inversions. The clear and coherent downward motion before, and the upward step coinciding with the LP event are both masked by the filter and their implications for the source are lost when inverting only in this narrow frequency band.

5. Discussion

Near summit LP observations on both Turrialba and Etna volcanoes demonstrate that both single event recordings and stacks of numerous repeating events show step-like displacement waveforms, which present as wave "pulses" in velocity seismograms. Low cut filtering traditionally applied prior to waveform inversion does not preserve these displace-

ment signals, compromising our assessment of the broadband source-time history. These step-like displacement signals are only seen in the near-field region from the source, consistent with theoretical displacement fields for dislocations [e.g. *Okada*, 1992]. The near- and intermediate-field terms, containing static deformation signals, decay much faster with the source-receiver distance than the purely dynamic far-field term [for details, see *Lokmer and Bean*, 2010]. As a consequence, the step signal can rapidly fall under the detection threshold (around 1 μm on 3ESPCD instruments) within a distance of approximately 1-2 km from the source.

The results from our laboratory experiments show that the detection of static displacements is primarily controlled by the SNR. Moving median filters on broadband data can reduce long-period noise whilst retaining static displacements. Common methods of displacement detection, such as GPS or InSAR do not offer the resolution (both methods have their limits around 1-10 mm [e.g. *Fournier et al.*, 2011; *Bürgmann et al.*, 2000]) needed to resolve steps of such small magnitude (order of 1-10 μm in our experiments) and short time history. In some scenarios, a comparison of inferred steps with long-term deformations measured with GPS or InSAR could be of interest in order to investigate a possible accumulation of such steps. However, a seismometer (and thus the method) is not directly sensitive to such long-term deformation.

Generally, inversions carried out using bandpass filtered seismograms result in a bandpass filtered time history of the source. If the time history of the actual source process differs from a zero-mean transient motion, the source time function obtained from filtered inversions will significantly differ from the real scenario. For example, a pure ramp

function (as might be expected for fault slip) is transformed into a zero-mean pulse with positive and negative lobes when subjected to a bandpass filter and its static displacement component is lost during filtering. Thus, source time functions obtained from band-limited inversions should always be interpreted as a filtered version of the true displacement and not as a complete history of the source motion. Otherwise, the underlying source process may be misinterpreted.

6. Conclusions

We have successfully recovered static displacement steps from field and laboratory seismometer data by applying median filters to reduce long period noise and long term instrument trends. The performance of this method is limited by the size of the step signal in relation to the long period noise, but is applied successfully to signals comparable to real world examples. Using field data from Turrialba volcano, Costa Rica, we recovered steps associated with LP events; stacks of many events show that this is coherent across many similar events. On Mt Etna, LP events also show a step-like behaviour embedded in a longer period signal, which is masked by traditional bandpass filters used for LP analysis.

A more detailed analysis of these new observations, including source inversions, is beyond the scope of this study. Hence we do not attempt to relate the surface waveforms directly to source models here. However, our results show that we are missing important information on LP sources if we analyse only the most energetic part of the recordings. The new observations reported in this paper pave the path for a more detailed analysis of LP sources from existing and future datasets. Additionally, this work shows that near field broad band observations are important in order to gain a more complete image of volcano

seismic sources. A more considered approach to waveform analysis demonstrates that even in relatively noisy volcanic environments we can access subtle information, which might fundamentally change our interpretation of underlying source processes.

Acknowledgments. The research leading to these results has received funding from the People Programme (Marie Curie Actions) of the European Union's Seventh Framework Programme (FP7/2007-2013) under the project NEMOH, REA grant agreement n° 289976. The data from laboratory and Turrialba experiments can be obtained from the corresponding author via e-mail. We are grateful to D. Patanè and L. Zuccarello (INGV Catania) for providing Etna data, which is subject to INGV's data policy. F. Martini, M. Mora, J. Pacheco are acknowledged for their contributions to the field experiment on Turrialba. Thanks to T. Ferreira, A. Garcia (CVARG, Azores), F. Heffernan (who enthusiastically built the step table) and M. Möllhoff (UCD) for support with the lab experiments. We thank N. Fournier and an anonymous reviewer for their comments which helped to improve the paper. Data processing was aided by ObsPy toolbox [*Beyreuther et al.*, 2010].

References

Bean, C. J., L. De Barros, I. Lokmer, J.-P. Metaxian, G. O' Brien, and S. Murphy (2014), Long-period seismicity in the shallow volcanic edifice formed from slow-rupture earthquakes, *Nature Geoscience*, *7*(1), 71–75.

Beyreuther, M., R. Barsch, L. Krischer, T. Megies, Y. Behr, and J. Wassermann (2010), ObsPy: A Python Toolbox for Seismology, *Seismological Research Letters*, *81*(3), 530–

533, doi:10.1785/gssrl.81.3.530.

Bürgmann, R., P. A. Rosen, and E. J. Fielding (2000), Synthetic aperture radar interferometry to measure earth's surface topography and its deformation, *Annual Review of Earth and Planetary Sciences*, *28*(1), 169–209, doi:10.1146/annurev.earth.28.1.169.

Chanerley, a. a., N. a. Alexander, J. Berrill, H. Avery, B. Halldorsson, and R. Sigbjornsson (2013), Concerning Baseline Errors in the Form of Acceleration Transients When Recovering Displacements from Strong Motion Records Using the Undecimated Wavelet Transform, *Bulletin of the Seismological Society of America*, *103*(1), 283–295, doi:10.1785/0120110352.

Chouet, B. (1986), Dynamics of a fluid-driven crack in three dimensions by the finite difference method, *Journal of Geophysical Research*, *91*, 13,967, doi:10.1029/JB091iB14p13967.

Chouet, B. (2003), Volcano Seismology, *Pure and Applied Geophysics*, *160*(3), 739–788, doi:10.1007/PL00012556.

Cusano, P., S. Petrosino, and G. Saccorotti (2008), Hydrothermal origin for sustained Long-Period (LP) activity at Campi Flegrei Volcanic Complex, Italy, *Journal of Volcanology and Geothermal Research*, *177*(4), 1035–1044, doi:10.1016/j.jvolgeores.2008.07.019.

De Barros, L., I. Lokmer, C. J. Bean, G. S. O'Brien, G. Saccorotti, J.-P. Métaxian, L. Zuccarello, and D. Patanè (2011), Source mechanism of long-period events recorded by a high-density seismic network during the 2008 eruption on Mount Etna, *Journal of Geophysical Research*, *116*(B1), B01,304, doi:10.1029/2010JB007629.

Eyre, T. S., C. J. Bean, L. De Barros, G. S. O'Brien, F. Martini, I. Lokmer, M. M. Mora, J. F. Pacheco, and G. J. Soto (2013), Moment tensor inversion for the source location and mechanism of long period (LP) seismic events from 2009 at Turrialba volcano, Costa Rica, *Journal of Volcanology and Geothermal Research*, *258*, 215–223, doi:10.1016/j.jvolgeores.2013.04.016.

Eyre, T. S., C. J. Bean, L. De Barros, F. Martini, I. Lokmer, M. M. Mora, J. F. Pacheco, and G. J. Soto (2015), A brittle failure model for long-period seismic events recorded at turrialba volcano, costa rica, *Journal of Geophysical Research: Solid Earth*, pp. n/a–n/a, doi:10.1002/2014JB011108.

Ferrazzini, V., and K. Aki (1987), Slow waves trapped in a fluid-filled infinite crack: Implication for volcanic tremor, *Journal of Geophysical Research*, *92*(2), 9215, doi:10.1029/JB092iB09p09215.

Fournier, N., A. D. Jolly, and C. Miller (2011), Ghost tilt signal during transient ground surface deformation events: Insights from the September 3, 2010 Mw7.1 Darfield earthquake, New Zealand, *Geophysical Research Letters*, *38*(16), 1–5, doi:10.1029/2011GL048136.

Graizer, V. M. (2005), Effect of tilt on strong motion data processing, *Soil Dynamics and Earthquake Engineering*, *25*(3), 197–204, doi:10.1016/j.soildyn.2004.10.008.

Kinoshita, S. (2008), Tilt Measurement Using Broadband Velocity Seismograms, *Bulletin of the Seismological Society of America*, *98*(4), 1887–1897, doi:10.1785/0120070230.

Kumagai, H. (2002), Waveform inversion of oscillatory signatures in long-period events beneath volcanoes, *Journal of Geophysical Research*, *107*, 1–13, doi:

10.1029/2001JB001704.

Kumagai, H., B. a. Chouet, and P. B. Dawson (2005), Source process of a long-period event at Kilauea volcano, Hawaii, *Geophysical Journal International*, *161*, 243–254, doi:10.1111/j.1365-246X.2005.02502.x.

Legrand, D., S. Kaneshima, and H. Kawakatsu (2000), Moment tensor analysis of near-field broadband waveforms observed at Aso volcano, Japan, *Journal of Volcanology and Geothermal Research*, *101*, 155–169, doi:10.1016/S0377-0273(00)00167-0.

Lokmer, I., and C. J. Bean (2010), Properties of the near-field term and its effect on polarisation analysis and source locations of long-period (LP) and very-long-period (VLP) seismic events at volcanoes, *Journal of Volcanology and Geothermal Research*, *192*(1-2), 35–47, doi:10.1016/j.jvolgeores.2010.02.008.

Lokmer, I., C. J. Bean, G. Saccorotti, and D. Patanè (2007), Moment-tensor inversion of LP events recorded on Etna in 2004 using constraints obtained from wave simulation tests, *Geophysical Research Letters*, *34*(22), L22,316, doi:10.1029/2007GL031902.

Lokmer, I., G. Saccorotti, B. Di Lieto, and C. J. Bean (2008), Temporal evolution of long-period seismicity at Etna Volcano, Italy, and its relationships with the 20042005 eruption, *Earth and Planetary Science Letters*, *266*(1-2), 205–220, doi:10.1016/j.epsl.2007.11.017.

McNutt, S. R. (2005), Volcanic Seismology, *Annual Review of Earth and Planetary Sciences*, *33*(1), 461–491, doi:10.1146/annurev.earth.33.092203.122459.

Nakano, M., H. Kumagai, and B. a. Chouet (2003), Source mechanism of long-period events at Kusatsu-Shirane Volcano, Japan, inferred from waveform inversion of the

effective excitation functions, *Journal of Volcanology and Geothermal Research*, *122*, 149–164, doi:10.1016/S0377-0273(02)00499-7.

Neuberg, J., R. Luckett, B. Baptie, and K. Olsen (2000), Models of tremor and low-frequency earthquake swarms on Montserrat, *Journal of Volcanology and Geothermal Research*, *101*, 83–104, doi:10.1016/S0377-0273(00)00169-4.

Okada, Y. (1992), Internal deformation due to shear and tensile faults in a half-space, *Bulletin of the Seismological Society of America*, *82*(2), 1018–1040.

Pillet, R., and J. Virieux (2007), The effects of seismic rotations on inertial sensors, *Geophysical Journal International*, *171*(3), 1314–1323, doi:10.1111/j.1365-246X.2007.03617.x.

Rodgers, P. W. (1968), The Response of the Horizontal Pendulum Seismometer to Rayleigh and Love Waves, Tilts and Free Oszillations of the Earth, *Bulletin of the Seismological Society of America*, *58*(5).

Schreiber, K. U., G. E. Stedman, H. Igel, and A. Flaws (2006), Ring laser gyroscopes as rotation sensors for seismic wave studies, in *Earthquake Source Asymmetry, Structural Media and Rotation Effects*, edited by R. Teisseyre, E. Majewski, and M. Takeo, pp. 377–390, Springer Berlin Heidelberg, doi:10.1007/3-540-31337-0_29.

Wielandt, E., and T. Forbriger (1999), Near-field seismic displacement and tilt associated with the explosive activity of Stromboli, *Annals of Geophysics*, *42*(3), 407–416, doi:10.4401/ag-3723.

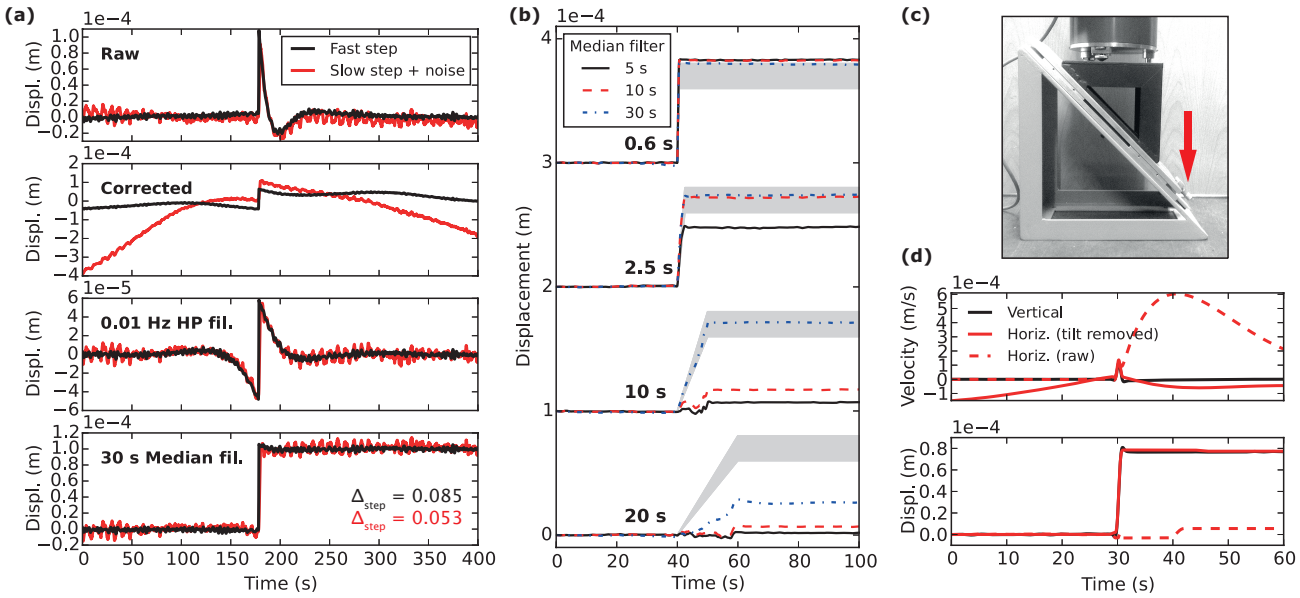

Figure 1. (a) Recovery of a vertical 94 μm step recorded on a Lennartz step table. Black: 0.6 s ramp time; red: 1.8 s ramp time and added field data noise. The step is masked by the bandpass filter, moving median filters can reduce noise without masking the step. (b) Recovery of vertical steps with varying ramp lengths and median filter windows, recorded on customized step table. Grey area indicates the actual displacement including errors. (c) Customized step table, allowing for ramps of varying amplitudes and rise times; the arrow marks the micrometer screw used to control the displacement. (d) Recovery of a horizontal step contaminated with tilt. When tilt is reduced [following *Wielandt and Forbriger*, 1999], the horizontal step aligns well with the identical vertical step (as seismometer displacements in horizontal and vertical directions are equal).

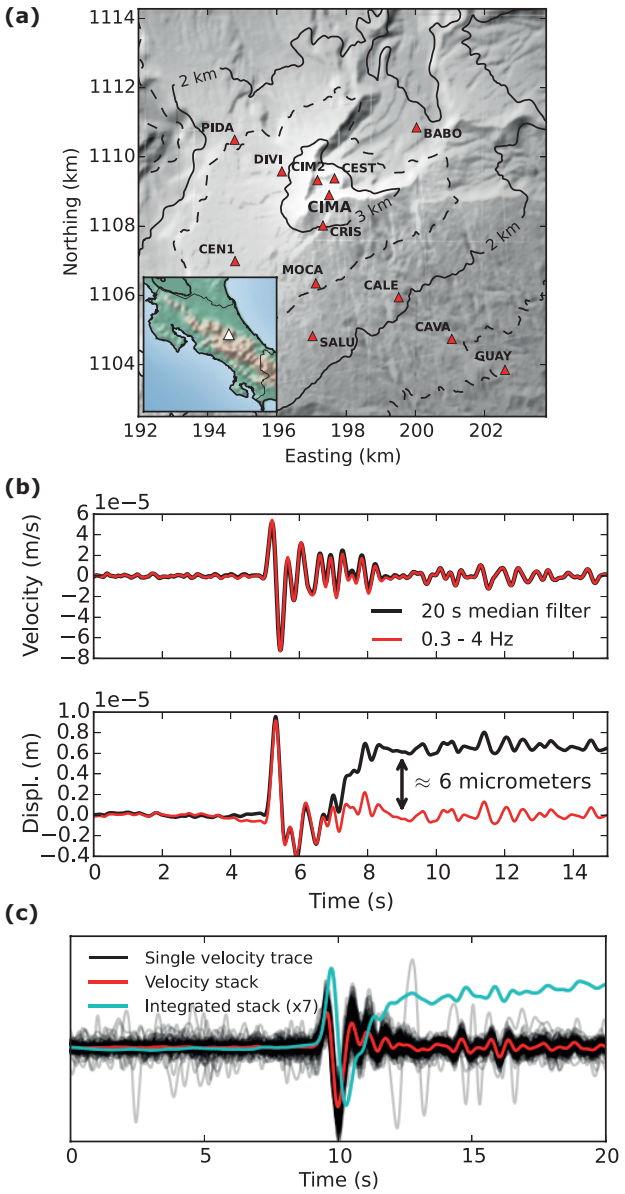

Figure 2. (a) Station locations on Turrialba volcano in 2009. Inset shows the location of the volcano within Costa Rica. (b) Top: Vertical LP event seismogram from Turrialba, recorded on Turrialba station CIMA in 2009, processed with median filter (20 s) or bandpass filter (0.3 - 4 Hz); Bottom: corresponding displacements; median filter processed data shows a step masked by the bandpass filter. (c) Stack of 183 unfiltered, instrument corrected and normalised LP events from a family at station CIMA. Due to the high S/N ratio in the stack, a step similar to the single event in (b) is visible in the unprocessed integrated stack.

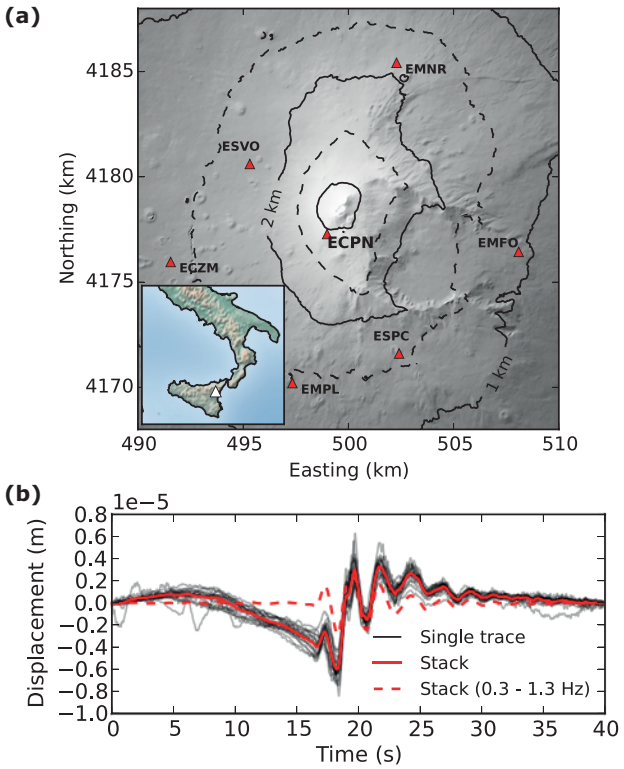

Figure 3. (a) Permanent broadband station locations on Mt Etna in 2005. Inset shows the location of the volcano within Southern Italy. (b) Vertical displacements from 17 LP events on Etna, recorded on summit station ECPN and stack, showing step-like behaviour embedded in a longer period signal, not recovered in the filtered representation.